Int. J. Radiation Oncology Biol. Phys., Vol. 60, No. 5, pp. 1589–1601, 2004

0360-3016/04/$–see front matter

ELSEVIER

doi:10.1016/j.ijrobp.2004.07.712

PHYSICS CONTRIBUTION

COMPARISON OF RECTAL DOSE–WALL HISTOGRAM VERSUS DOSE–VOLUME HISTOGRAM FOR MODELING THE INCIDENCE OF LATE RECTAL BLEEDING AFTER RADIOTHERAPY

Susan L. Tucker, Ph.D.,* Lei Dong, Ph.D.,† Rex Cheung, M.D., Ph.D.,‡ Jennifer Johnson, M.S.,† Radhe Mohan, Ph.D.,† Eugene H. Huang, M.D.,‡ H. Helen Liu, Ph.D.,† Howard D. Thames, Ph.D.,* and Deborah Kuban, M.D.‡

Departments of *Biostatistics and Applied Mathematics, †Radiation Physics, and ‡Radiation Oncology, The University of Texas M.D. Anderson Cancer Center, Houston, TX

Purpose: To compare the fits of normal-tissue complication probability (NTCP) models based on rectal dose–wall histograms (DWHs) vs. dose–volume histograms (DVHs) when the two are used to analyze a common set of late rectal toxicity data.

Methods and Materials: Data were analyzed from 128 prostate cancer patients treated with 3-dimensional conformal radiotherapy (3D-CRT) at The University of Texas M.D. Anderson Cancer Center (UTMDACC). The DVH for total rectal volume, including contents, was obtained for each patient from the treatment-planning system. A DWH was also computed, using the outer rectal contour plus an autogenerated inner contour that corresponds to an assumed 3-mm rectal wall thickness. The endpoint for analysis was Grade 2 or higher late rectal bleeding within 2 years of treatment; all patients had at least 2 years of follow-up. Four different NTCP models were fitted to the response data by using either the DVH or the DWH to describe the dose distribution to rectum or rectal wall, respectively. The 4 models considered were the Lyman model, the mean dose model, the parallel-architecture model, and a model based on the volume of a organ receiving more than a specified dose (the "cutoff-dose" model).

Results: For each of the models, the fit to the late rectal bleeding data was slightly improved when the analysis was based on the rectal DWH instead of on the DVH. In addition, the results of the cutoff dose and parallel architecture models were consistent with one another for the DWH data but not for the DVH data. For the DWH data, both models predict a 50% or higher incidence of Grade 2 or worse late rectal bleeding within 2 years if 80% or more of the rectal wall is exposed to doses greater than 32 Gy. A 50% or higher incidence of rectal bleeding is also predicted if the mean dose to rectal wall exceeds 53.2 Gy.

Conclusions: A consistent, although modest, improvement occurs in the fits of NTCP models to the UTMDACC 2-year late rectal bleeding data when the fit is based on the rectal dose–wall histogram instead of on the dose–volume histogram for entire rectum, including contents.

Dose–wall histogram, Dose–volume histogram, Rectal toxicity, Normal-tissue complication probability, Prostate cancer.

INTRODUCTION

The rationale for 3-dimensional conformal radiotherapy (3D-CRT) and intensity-modulated radiotherapy (IMRT) is that safe dose escalation to tumors may be achievable if the volume of adjacent normal tissue exposed to high radiation doses can be kept within acceptable limits. To understand these limits in terms of dose and volume, many studies have been performed to estimate the risk of normal-tissue complications as a function of the dose distribution to tissue summarized in the form of a dose–volume histogram (DVH) (1–14). Although the DVH does not retain spatial information (i.e., which part of the organ is exposed to which dose), it nonetheless provides considerable information regarding the dose–volume characteristics of the treatment plan.

For "solid" organs, such as liver, lung, and parotids, use of a DVH based on the entire volume encompassed by the outer contour of the organ makes sense as a way of summarizing the dose–volume distribution. However, for "hollow" organs, such as rectum and bladder, the contents of the organ are irrelevant to the risk of complications that may occur as a result of radiotherapy (RT). For this reason, the dose–wall histogram and dose–surface histogram (DSH)

Reprint requests to: Susan L. Tucker, Ph.D., Department of Biostatistics and Applied Mathematics, The University of Texas M.D. Anderson Cancer Center, 1515 Holcombe Blvd, Unit 237, Houston, TX 77030. Tel: (713) 792-2613; Fax: (713) 792-4262; E-mail: sltucker@mdanderson.org

Received Apr 4, 2004, and in revised form Jul 12, 2004. Accepted for publication Jul 14, 2004.

have been proposed as alternatives to the DVH for such organs (15–19). The rectal DWH describes the dose distribution to the 3D volume enclosed between the inner and outer surfaces of the rectal wall, whereas the DSH describes the dose distribution to the 2-dimensional (2D) surface defined by the inner or outer rectal contour only.

Although the outer rectal contour is easily recognized on CT scans, accurate delineation of the inner surface of the rectal wall can be quite difficult because of the similarity in CT numbers for rectal tissue and solid rectal contents. This circumstance makes manual contouring of the entire rectal wall subject to considerable uncertainty, in addition to being labor intensive. One proposed solution is to estimate the location of the inner contour on the basis of an assumed wall thickness such as 3 mm (20). In actuality, the thickness of the rectal wall probably varies with the degree of rectal distension; its thickness is at maximum when the rectum is empty and decreases as distension increases (19). However, a reasonable expectation is that use of a fixed wall thickness would provide a good first approximation of the true DWH and could lead to an improvement in describing the rectal dose distribution, compared with use of the DVH for rectum viewed as a solid organ.

At first glance, the notion that NTCP models based on the DWH would better describe the risk of rectal toxicity than do models based on the DVH seems intuitively clear because of the irrelevance of the dose received by the rectal contents. However, the DWH assessed from the planning CT is not necessarily an accurate representation of the true dose distribution to rectal wall during treatment. Numerous studies have demonstrated that considerable variation may occur in the shape and position of internal organs, including rectum, during the course of RT for prostate cancer (21–31). This variation is largely caused by interfractional differences in rectal and bladder filling over the course of treatment. In addition, the DVH and DWH have fairly similar shapes (16, 17, 19). Therefore, whether NTCP modeling based on the DWH (especially a semiauto-contoured DWH) would in fact be more accurate than NTCP modeling based on the DVH is not immediately obvious.

The aim of the present study was to investigate the extent of improvement, if any, in the predictive power of NTCP models fitted to rectal toxicity data by use of a semiauto-contoured DWH in place of the DVH for describing the dose–volume distribution to rectum, on the basis of the planning CT. In previous studies, we used rectal DVH data from patients treated with 3D-CRT for prostate cancer at UTMDACC to fit 5 different NTCP models that described the 2-year incidence of Grade 2 or higher late rectal bleeding as a function of the dose–volume distribution to rectum as a solid organ, including contents (32, 33). In the present study, we have reanalyzed the same set of clinical-response data by use of semiauto-contoured dose–wall histograms generated from the outer contour of the rectum by assuming a fixed 3-mm wall thickness, and we have refitted 4 of the 5 NTCP models considered previously. Initially our intention was to compare the resulting model fits directly to those obtained previously. However, for reasons explained below, the DVHs had to be recalculated for the purposes of comparison with the semiauto-contoured DWHs. Therefore, we have also refitted each of the NTCP models on the basis of the new DVHs.

METHODS

Patient population

The patient population in the present study is the same as in our 2 previous modeling studies of rectal toxicity (32, 33) and comprises 128 patients who were treated for localized, biopsy-confirmed prostate cancer with definitive 3D-CRT at UTMDACC and had a minimum follow-up of 2 years. All of these patients were included in the 78-Gy arm of the UTMDACC dose-escalation trial (13, 34) and were treated with 46 Gy at 2 Gy per fraction to isocenter in a conventional 4-field box technique, followed by a 6-field 3D-CRT boost to 78 Gy in 2 lateral and 4 oblique fields. This retrospective data analysis was approved by the Institutional Review Board of the UTMDACC.

Assessment of rectal toxicity

Because all of the patients included in the present study were treated on an institutional dose-escalation protocol, they were scored prospectively for rectal toxicity. Follow-up examinations were performed every 6-months during the first 2 years after RT, and annually thereafter. Late rectal complications were defined as those that occur at least 6 months after completion of RT and were graded on a modified toxicity scale based on criteria from the Radiotherapy Oncology Group (35), the Late Effects Normal Tissue Task Force (36), and Fox Chase Cancer Center (37), as described in Table 1. Consistent with our two previous analyses (32, 33), the endpoint for the present data analysis was Grade 2 or higher late rectal bleeding within 2 years of treatment (yes/no). As in the previous studies, we also included 1 patient as a responder who experienced rectal bleeding at 5 months after RT instead of at 6 months or

Table 1. UTMDACC modified toxicity score for late rectal complications

Grade	Complication
1	Excess bowel movements twice baseline; slight rectal discharge or blood
2	Two or more antidiarrheals/week; two or fewer coagulations for bleeding; occasional steroids for ulceration; occasional dilation; intermittent use of incontinence pads; regular nonnarcotic or occasional narcotic for pain
3	Two or more antidiarrheals/day; three or more coagulations or any transfusion; prolonged steroids per enema; hyperbaric oxygen for bleeding/ulceration; regular dilation; persistent use of incontinence pads; regular narcotics for pain
4	Dysfunction requiring surgery; perforation; life-threatening bleeding

later. All patients in this cohort had at least 2 years of follow-up, so the status of the binary endpoint (yes/no) was known unambiguously for all patients.

Dose–wall histograms and dose–volume histograms

As in our previous studies (9, 32, 33), treatment plans were restored from the institutional archives and analyzed for each patient to obtain a DVH for the volume of rectum (including contents) enclosed within the outer rectal contour on each CT slice. The rectum was outlined from the sigmoid flexure to its inferiormost aspect near the level of the ischial tuberosities.

Of the 128 patients included in the present study, 14 patients had plans designed by our current Pinnacle treatment-planning system (Philips Medical Systems, Andover, MA). For these 14 patients, a computer program was written to generate an inner contour retracted from the outer contour by 2 mm, 3 mm, 4 mm, or 5 mm, and the semiautocontoured volume was taken as an approximation of the rectal wall. Pinnacle was used to calculate the dose distribution to the volume of rectum encompassed by the 2 contours and, thereby, produced an estimated DWH. The DWHs for each patient, calculated using different wall thicknesses (2–5 mm), were found to differ only slightly from one another, so all subsequent calculations used the 3-mm DWH only. The choice of the 3-mm wall thickness is also supported by the study of Rasmussen and Riis (38), in which rectal wall thicknesses measured by ultrasound were found to have a median of 2.6 mm, 2.8 mm, and 3.2 mm in 19 control subjects, 18 patients with Crohn's disease, and 33 patients with ulcerative colitis, respectively.

The remaining 114 patients had treatment plans designed by an earlier in-house system no longer in use. For these patients, the original treatment plan (dose matrix and contoured structures) was converted and imported into the Pinnacle treatment-planning system. DWHs were then computed as described above. In addition, the DVH was recomputed for comparison with the earlier DVH generated using the in-house system.

The dose bins for each DVH and DWH were 0.1 Gy in size. All doses represent total doses that have not been corrected for fractionation. Unless otherwise specified, the terms DVH and DWH are used here to refer to the relative DVH and DWH, normalized to 100% of the total contoured rectal volume or rectal wall volume, respectively.

NTCP models

Four different dose–volume response models were fitted to the late rectal bleeding data (Grade 2 or higher late rectal bleeding within 2 years of treatment: yes/no) by use of the dose–volume information from either the DVH or the DWH. These widely used models have been described in detail elsewhere (33). Briefly, each model is based on a summary measure μ extracted from the DVH or the DWH, which is then converted to a complication probability using a probit equation:

$$\mathrm{NTCP}(\mu) = \frac{1}{\sqrt{2\pi}} \int_{-\infty}^{s(\mu-\mu_{50})} \exp(-du^2/2)du \qquad (1)$$

Each of the models includes at least 2 unknown parameters, μ_{50} (determining the position of curve) and s (determining the slope of the curve and often written in the form s = (m · μ_{50})$^{-1}$, as well as any other parameters used to define the summary measure μ. The models considered here correspond to the following summary measures of the DVH or DWH:

Lyman model

For the Lyman model (39) combined with the Kutcher-Burman DVH-reduction scheme (40), μ is equal to the effective dose, defined by (41)

$$D_{\mathrm{eff}} = \left(\sum_i v_i \cdot D_i^{1/n}\right)^n \qquad (2)$$

where v_i is the volume of the dose bin that corresponds to dose D_i in the differential DVH or DWH. In addition to the parameters s and $\mu_{50} = D_{50}$, this model has a third parameter, n.

Mean dose model

For the mean dose model, the quantity μ is the mean dose (MD) to the organ:

$$MD = \sum_i v_i \cdot D_i \qquad (3)$$

This model includes only the 2 probit parameters s and $\mu_{50} = MD_{50}$ and is a special case of the Lyman model that corresponds to $n = 1$.

Cutoff-dose model

For the cutoff-dose model, μ represents the fractional volume VD_c of an organ receiving a dose greater than or equal to a "cutoff" dose D_c (for example V60 corresponds to the proportion of the organ receiving doses of 60 Gy or more):

$$VD_c = \sum_{i \ni (D_i \geq D_c)} v_i \qquad (4)$$

where the sum is over i such that $D_i \geq D_c$. This model has 3 parameters: the optimal cutoff dose, D_c, as well as the 2 probit parameters s and $\mu_{50} = VD_c(50)$.

Parallel model

For the parallel architecture model (42–44), a local-damage function, $P(D)$, is used to represent the probability of destroying organ function in a small subvolume of tissue exposed to dose D. We model $P(D)$ by use of a probit curve (Eq. 1) with parameters s_D corresponding to slope and D_{50} corresponding to position. The fraction of the organ dam-

aged by radiation, f_{dam}, is calculated by integrating the differential DVH or DWH against $P(D)$:

$$f_{dam} = \sum_i v_i \cdot P(D_i) \quad (5)$$

The quantity f_{dam} is the summary measure of the DVH or DWH that is then linked to complication probability by a second probit model (Eq. 1). We denote the parameters of this second probit curve by s_f and f_{50}. The parallel model used here, therefore, has 4 parameters: s_D, D_{50}, s_f, and f_{50}. The parallel model is a generalization of the cutoff-dose model in the sense that as the parameter s_D approaches infinity, the parallel model converges to the cutoff-dose model with $D_c = D_{50}$.

Each of the NTCP models described above was fitted by application of maximum-likelihood (ML) analysis (45) to the binary response data and to the dose-volume data for rectum plus contents (given by the DVH) or for rectal wall (given by the DWH). Confidence intervals for the ML parameter estimates were derived by use of the profile-likelihood method (45).

Model fits were compared according to the Akaike Information Criterion (AIC) (46, 47) or the area under the receiver-operating-characteristic (ROC) curve (48). The Akaike Information Criterion is defined as AIC = $-2 \cdot$ LL + $2 \cdot$ k, which adjusts the log-likelihood (LL) by the number of model parameters (k). The ROC curve is defined as the plot of sensitivity vs. 1 − specificity as the cutoff for predicting occurrence of a specified endpoint (in this case, Grade 2 or higher rectal bleeding within 2 years) is varied from NTCP = 0% to NTCP = 100%. The closer the area under the ROC curve (AUC) is to 1, the better the predictor. A random predictor, such as a coin toss, corresponds to AUC = 1/2.

RESULTS

Incidence of rectal bleeding

As described previously (32, 33), 29 of the 128 patients (23%) experienced Grade 2 or higher late rectal bleeding within 2 years of treatment. These 29 patients comprise all but 1 of the patients having Grade 2 or higher late rectal complications within 2 years of treatment; the remaining patient experienced Grade 2 diarrhea approximately 1 year after radiotherapy.

Dose–volume histograms and dose–wall histograms

The median length of contoured rectum measured vertically (i.e., not following the rectal curvature) was 11 cm (mean length, 10.9 cm). Because of individual variations in anatomy, rectal length varied from 8.5 to 15.6 cm, with an interquartile range of 9.0 to 12.6 cm and a standard deviation of 0.9 cm.

For the 114 patients with DVH data available from two different treatment-planning systems (Pinnacle vs. our earlier, in-house system; see *Methods* section), the cumulative DVHs were compared and found to differ at least slightly for all patients. Values of V40 (percent rectum exposed to doses of 40 Gy or more) differed by values that ranged up to 13% of rectum. Specifically, V40(Pinnacle) − V40(in-house system) ranged from −13.0% to 11.1% of rectum, with a median difference of −1.5%. The corresponding differences in rectal volume for V20 and V60 were −10.5% to 6.9% (median −2.5%) and −9.9% to 6.8% (median 0%), respectively. Because of the differences in DVH computed by the two different treatment-planning systems, and because Pinnacle was used to compute all DWHs, we elected, for consistency, to use only the DVH data from Pinnacle for all subsequent analyses in the present study. Model fits based on DVH data from our in-house treatment-planning system have been presented elsewhere (33).

Figure 1a shows the average cumulative DVH (cDVH) and cumulative DWH (cDWH) curves for rectum computed by the Pinnacle treatment-planning system for all 128 patients in the study. The cDWH curve lies below the cDVH curve for dose values in the range of 20 to 60 Gy, with the maximum difference of 5% occurring at 40 Gy. It lies above the cDVH curve over the dose range of 60 to 80 Gy. Again, the maximum difference is 5%, which occurs at 75.5 Gy. The pattern observed here, with the cDWH lying below the cDVH for intermediate doses but above the cDVH for the highest doses, has been reported elsewhere (15, 18).

Figure 1b illustrates the relationship between the average differential DVH (dDVH) and differential DWH (dDWH) curves for rectum computed by the Pinnacle treatment-planning system. The curves diverge at about 22 Gy, with the average dDWH curve lying above the average dDVH curve for doses in the range of 22 to 40 Gy and higher than 75 Gy and lying below the dDVH curve for doses in the range of 41 to 75 Gy. In particular, the dDWH curves are higher than the dDVH curves near both peaks of the differential–dose histograms, that is, near the dose values received by the largest subvolumes of solid rectum or rectal wall.

Figure 2 illustrates the average cumulative (panel a) and differential (panel b) rectal dose–wall histograms for the 29 patients who experienced Grade 2 or higher late rectal bleeding within 2 years of treatment vs. the 99 patients who did not. The average cDWH curve for the patients with bleeding lies above the cDWH curve for the nonbleeding patients throughout the entire dose range (0 to 80 Gy). In contrast, the average differential DWH curve for the bleeding patients does not lie consistently above the dDWH curve for the nonbleeding patients until the dose reaches about 38 Gy.

NTCP modeling

In view of the differences noted in the DVH data obtained by our two different treatment-planning systems, we refitted 4 of the 5 NTCP models investigated previously (32, 33) with the new (Pinnacle) DVH data derived for solid rectum, including contents. One of the models investigated previously, the cutoff-volume model, was not considered here because it was the poorest fitting model in our earlier study. The parameter estimates for the 4 refitted models are listed in Table 2.

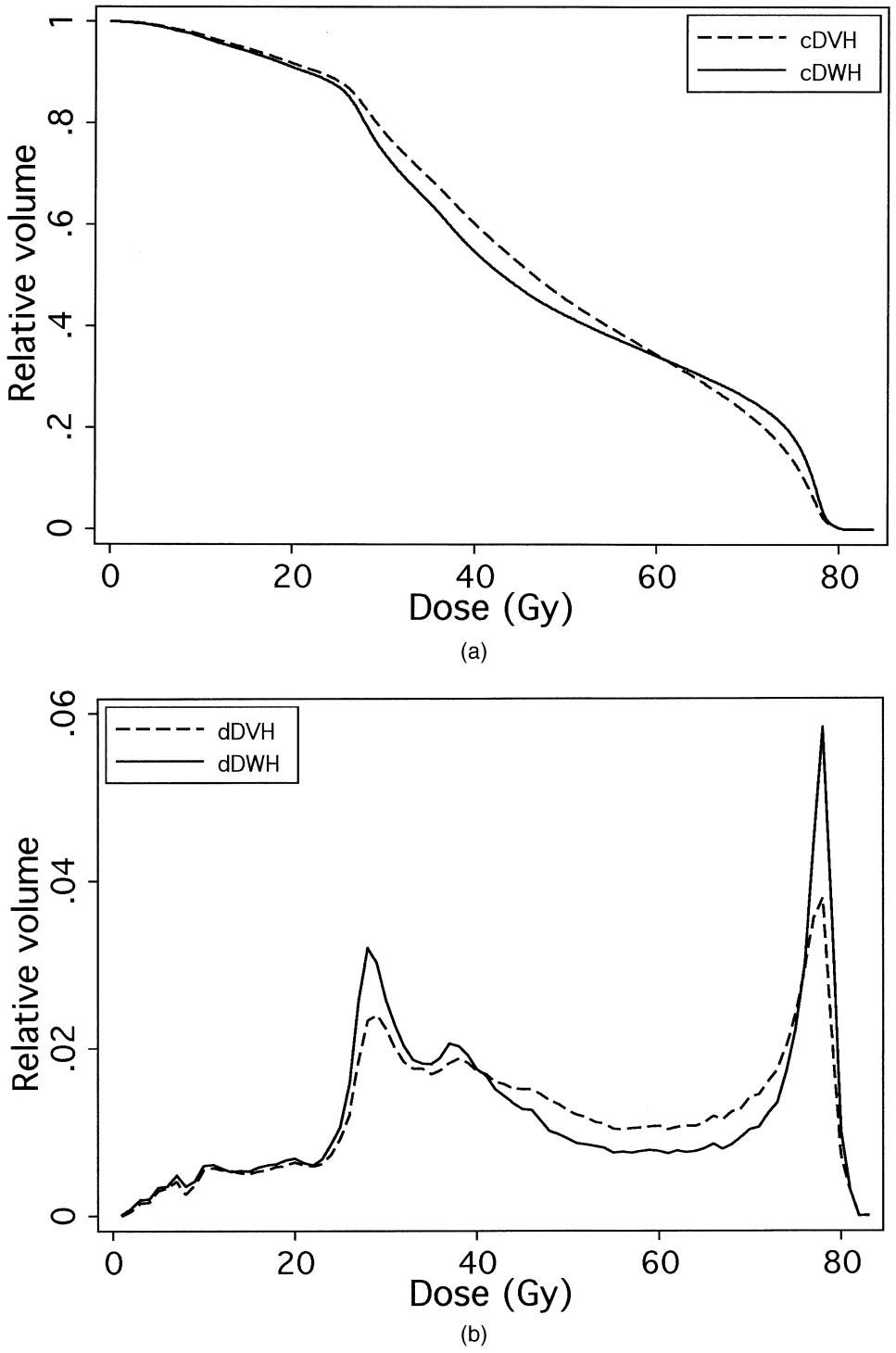

Fig. 1. (a) Average cumulative rectal dose volume histogram (DVH) and dose wall histogram (DWH) curves for all 128 patients in the study. Individual cDVH and cDWH curves were computed by the Pinnacle treatment-planning system and averaged at each dose point. (b) Average differential rectal DVH and DWH curves for all 128 patients in the study. Individual dDVH and dDWH curves were computed by the Pinnacle treatment-planning system and averaged at each dose point. For visual clarity (to reduce "jaggedness"), the dDVH and dDWH curves are plotted from the data at 1-Gy dose intervals.

Table 2 also lists the parameter estimates obtained by fitting each of the NTCP models to the late rectal bleeding data by substituting the DWH data for rectal wall in place of the DVH for solid rectum. Two interesting observations can be made from the results listed in Table 2.

First, for each of the NTCP models, a larger log-likeli-

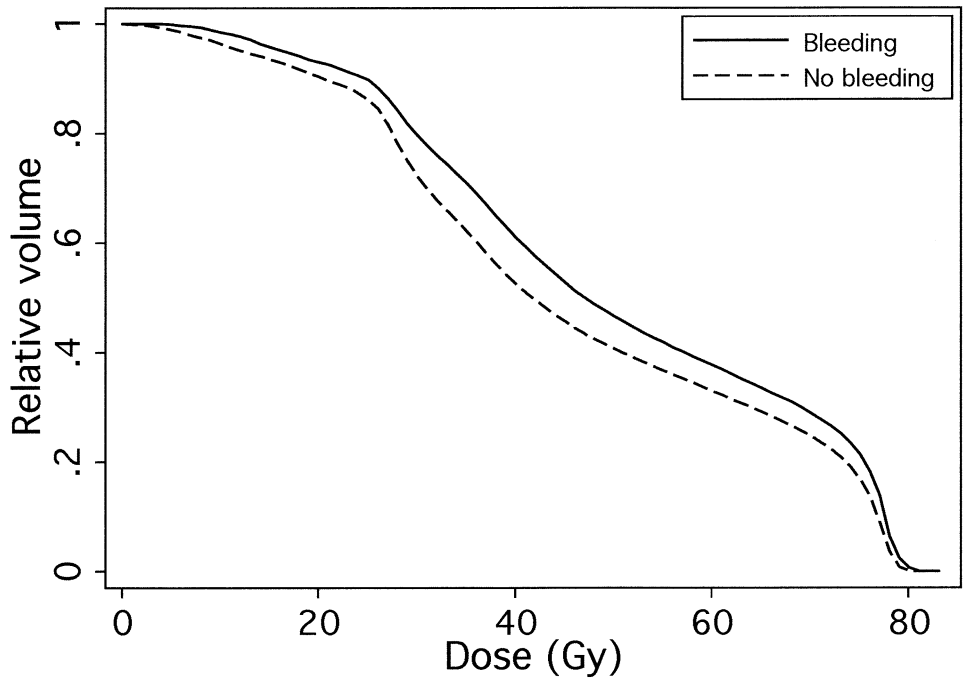

(a)

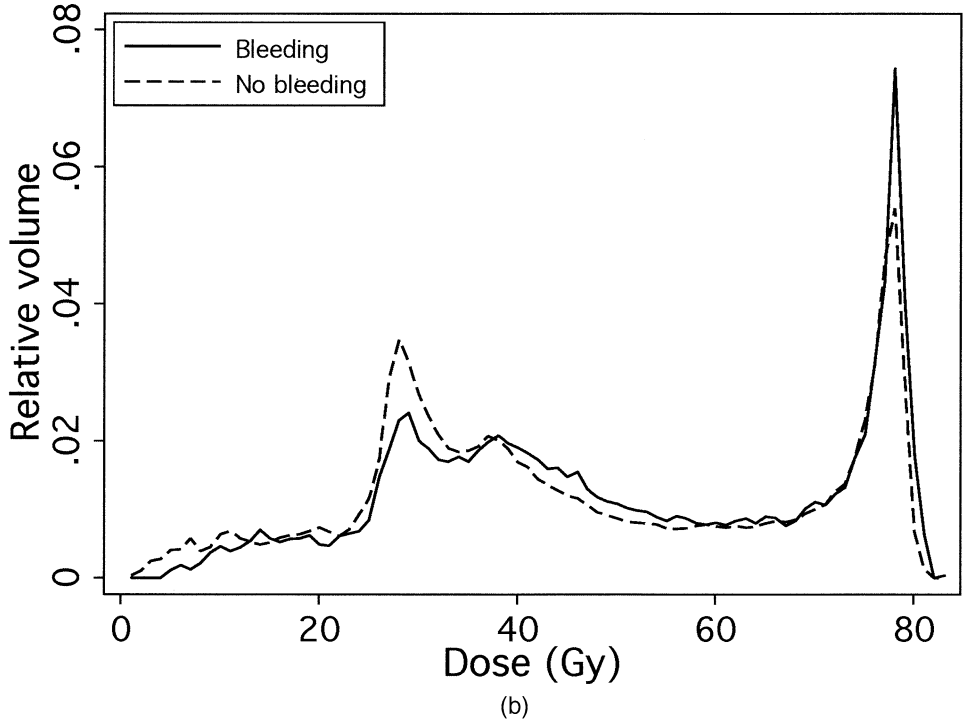

(b)

Fig. 2. Average cumulative (a) and differential (b) rectal dose wall histogram (DWH) curves for the patients with or without Grade 2 or higher late rectal bleeding within 2 years of treatment.

hood value was obtained for the model fit based on DWH data than for the model fit based on DVH data. Although no statistical comparison can be made, this finding indicates that the model fits based on DWH data are better than those based on DVH data.

Second, the optimal cutoff dose, $D_c = 32.4$ Gy, estimated from the fit of the cutoff dose model by use of the DWH data, is very close to the estimate of the dose corresponding to 50% local damage in the parallel model, $D_{50} = 32.7$ Gy. Similarly, the estimated volumes of injured rectal wall corresponding to a 50% risk of Grade 2 or higher late rectal bleeding are very similar for the two models. The cutoff-dose model predicts a 50% risk of rectal bleeding if 81.7% of the rectal wall receives a dose of 32.4 Gy or higher,

Table 2. Comparison of NTCP model fits to DVH versus DWH data

Model	Parameter	DVH data	DWH data
Lyman	$\log_{10} n$	0.013 (−1.55, 5.47)	4.95 (−0.35, 5.50)
	m	0.160 (0.039, 0.398)	0.167 (0.089, 0.300)
	D_{50} (Gy)	55.9 (49.0, 75.8)	48.6 (46.1, 58.4)
	LL	−60.47	−57.72
Mean dose	MD_{50} (Gy)	56.0 (53.1, 63.2)	53.2 (51.2, 57.7)
	s (Gy^{-1})	0.112 (0.056, 0.174)	0.154 (0.083, 0.230)
	LL	−60.47	−58.48
Cutoff dose	D_c (Gy)	44.8 (29.4, 76.8)	32.4 (28.2, 47.1)
	VD_c (50) (%)	69.7 (17.8, 97.9)	81.7 (56.0, 92.4)
	s	4.91 (2.38, 7.91)	7.11 (3.67, 10.9)
	LL	−60.90	−57.92
Parallel model	S_D (Gy^{-1})	0.008 (0, ∞)	0.132 (0.003, ∞)
	D_{50} (Gy)	4.92 (0, ∞)	32.7 (0, ∞)
	s_f	38.0 (2.69, ∞)	8.80 (3.84, ∞)
	f_{50}	0.655 (0.510, 1)	0.795 (0.076, 0.924)
	LL	−60.46	−57.83

Abbreviations: DVH = dose–volume histogram; DWH = dose–wall histogram; NTCP = normal tissue complication probability.

whereas the parallel model predicts a 50% risk of rectal bleeding if the fraction of damaged rectal wall, f_{dam} (defined by Eq. 5), is 79.5%. This result illustrates that the fits of the cutoff-dose model and the parallel model are remarkably consistent with one another when the DWH data are used. In theory, these two models should be consistent with one another because the parallel model converges to the cutoff-dose model when the local-damage curve is estimated to be steep. For the DVH data, however, no consistency in the fits of the two models is seen (cf. Table 2).

Figure 3 illustrates the calculation of the 95% profile-likelihood confidence interval for the maximum-likelihood estimate D_c = 32.4 Gy obtained from the cutoff-dose model by use of the DWH data. For each possible cutoff dose from 5 to

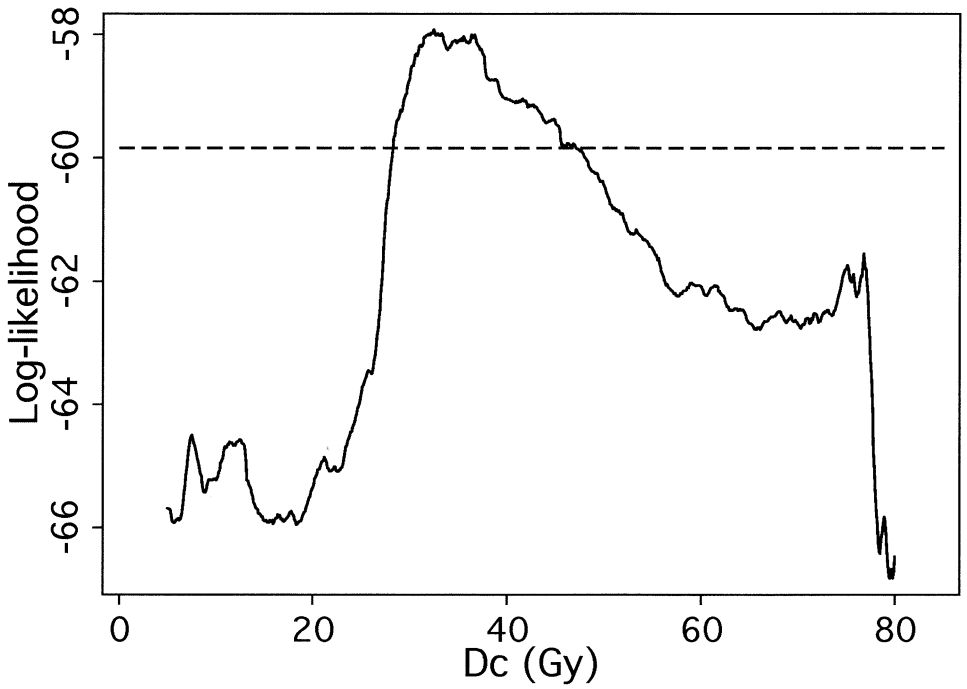

Fig. 3. Profile likelihood for the parameter D_c from the cutoff-dose model fitted to the dose wall histogram data. The solid curve shows the log-likelihood plotted against cutoff dose for values of D_c ranging from 5 to 80 Gy in increments of 0.1 Gy. The maximum likelihood (ML) estimate of D_c corresponds to the peak (maximum LL) at D_c = 32.4 Gy. The 95% profile-likelihood confidence interval corresponds to values of D_c for which the likelihood lies above the dashed line and ranges from 28 to 47 Gy.

80 Gy, in increments of 0.1 Gy, the rectal bleeding data were modeled as a probit function (Eq. 1) of VD_c by application of ML analysis. VD_c represents the percentage of rectal wall receiving doses of D_c Gy or more. The solid curve in Fig. 3 (the profile likelihood) shows the log-likelihood from each ML fit plotted as a function of cutoff dose, D_c. The peak, that is, the largest value of LL, occurs at $D_c = 32.4$ Gy, which, therefore, represents the ML estimate of D_c. The dashed horizontal line is displaced downward from the peak by a distance determined from the chi-square distribution (45); values of D_c that corresponding to LL values above the dashed line lie within the 95% profile-likelihood confidence interval for $D_c = 32.4$ Gy. As shown, the 95% confidence interval is relatively narrow and extends from 28.2 to 47.1 Gy.

In contrast, Table 2 indicates that the 95% confidence interval for the parameter D_{50} in the parallel model is extremely wide and encompasses all doses to rectal wall in this study (0 to 80 Gy). Nonetheless, in the fit of the parallel model to DWH data, a marked preference is seen for estimates of D_{50} near 32.7 Gy, compared with other values of D_{50}. This finding is illustrated in Fig. 4, which shows the profile likelihood for D_{50} from the parallel model. A pronounced peak is seen in the profile likelihood near $D_{50} = 32.7$ Gy. Although the horizontal line that represents the 95% confidence interval (not shown) lies entirely below the curve in Fig. 4, the line that represents the 55% confidence interval (dashed line in Fig. 4) defines a relatively narrow range of doses, from 22 to 38 Gy.

Table 3 lists the AIC and the AUC for each of the NTCP models fitted using the rectal DVH or DWH data. Although no statistical comparisons can be made, smaller values of AIC indicate better model fits, as do larger values of AUC. Table 3 shows that for each model, the fit was improved when the DWH data were used in the analysis instead of the DVH data.

Table 3 also shows that the best-fitting model, overall, was the simplest of the models considered, namely the 2-parameter mean-dose model. Fitting the mean-dose model to the DWH data yielded the smallest AIC and the largest AUC overall.

However, the differences among the model fits described in Table 2 are quite modest. This result is a consequence of the fact that the summary measures of the DWH that correspond to the various models were highly correlated; all pairwise correlation coefficients among mean dose, V32.4, D_{eff}, and f_{dam} were in the range of $r = 0.83$ to $r = 0.98$, with a significance level of $p < 0.0001$ in each case. Figure 5 shows the correlation between mean dose to rectal wall and V32.4 ($r = 0.90$). Converted to a probability scale, mean doses of 40, 45, 50, 55, and 60 Gy correspond to NTCP estimates of 2%, 10%, 31%, 61%, and 85%, respectively.

The tight correlations among mean dose, V32.4, and other variables listed above are a consequence of the patient treatment plans in the present study and may not be valid for patients with different plans. For example, if additional patients were treated so that 80% of the rectal wall received 32.4 Gy and 20% received 0 Gy, then the mean dose to rectal wall for those patients would be 26 Gy, and the correlation between V32.4 and mean dose in Fig. 5 would no longer hold. This example illustrates that the similarities among the model fits observed in this study are not expected

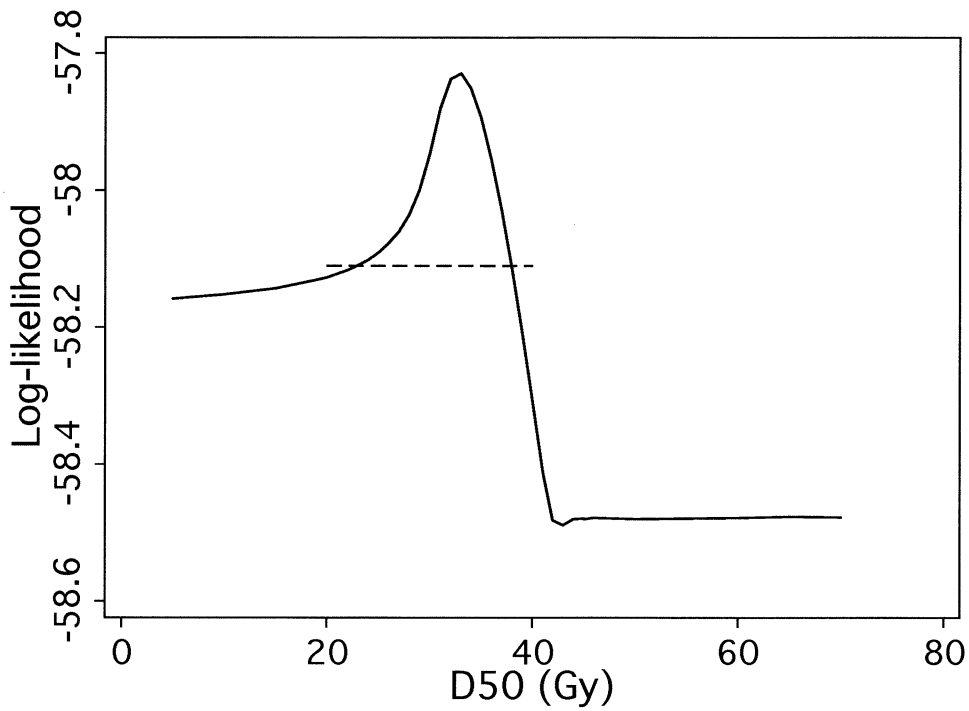

Fig. 4. Profile likelihood for the parameter D_{50} of the parallel model fitted by use of the dose wall histogram (DWH) data. The dashed line intersects the profile likelihood at points that define the 55% confidence interval for D_{50}.

Table 3. Akaike Information Criterion and area under the ROC curve computed from model fits to rectal DVH or DWH data

Model	AIC		AUC	
	DVH	DWH	DVH	DWH
Lyman model	126.9	121.4	0.731	0.763
Mean-dose model	124.9	121.0	0.733	0.765
Cutoff-dose model	127.8	121.8	0.727	0.761
Parallel model	128.9	123.7	0.731	0.759

Abbreviations: AIC = Akaike Information Criterion; AUC = area under curve; DVH = dose–volume histogram; DWH = dose–wall histogram; ROC = receiver operating characteristic.

to hold in general, in the presence of substantial differences in treatment plans from patient to patient.

DISCUSSION

The aim of the present study was to investigate whether NTCP models based on rectal dose–wall histograms, computed from the outer rectal contour plus an auto-generated inner contour that corresponds to a fixed wall thickness, could describe the incidence of late rectal bleeding better than NTCP models fitted by use of DVH data for solid rectum, including contents. Late rectal bleeding data from a cohort of 128 prostate cancer patients treated with 3D-CRT at UTMDACC were analyzed. The results of our study suggest a consistent, albeit modest, improvement in the fit of each of the NTCP models examined, when based on semiauto-contoured 3-mm DWH data instead of on DVH data.

Koper *et al*. (11) have also reported that rectal bleeding was more strongly associated, in their study, with dose–volume quantities derived from the rectal DWH than from the DVH . In contrast, Dale *et al*. (4) reported better correlations with the DVH. However, the study by Dale *et al*. (4) used a different toxicity endpoint; they computed a composite score based on patient responses to a questionnaire concerning 5 other symptoms (diarrhea, mucus discharge, pain, cramps, and gas) in addition to rectal bleeding. Moreover, the composite toxicity scores were compared with dose–volume parameters by application of Spearman correlation analysis, and the correlation coefficients were in all cases very low, which indicates, at most, a weak correlation with toxicity for both the DVH and the DWH data.

The degree of improvement that resulted from use of the DWH in lieu of the DVH in the present study is illustrated in Fig. 6. The mean dose to rectal wall is plotted against the mean dose to solid rectum for each patient in the study. Closed symbols correspond to patients with late rectal bleeding and open symbols correspond to patients without bleeding. The mean doses to the two structures are very similar, as indicated by the proximity of the data points to the dotted line that represents equality of mean dose to solid rectum and rectal wall. On average, the mean dose to rectal wall is within 2% of the mean dose to solid rectum, ranging

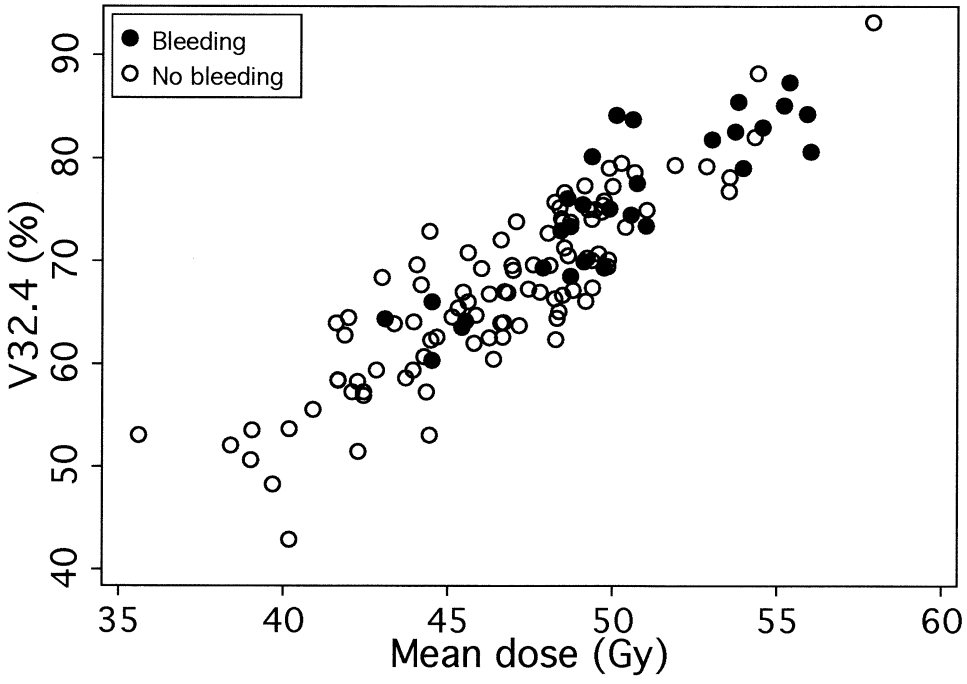

Fig. 5. Correlation between mean dose and V32.4 computed from the dose wall histogram (DWH) data for each of the 128 patients in the study. Solid symbols indicate data from patients who experienced late rectal bleeding within 2 years of treatment. Mean rectal wall doses of 40, 45, 50, 55, and 60 Gy correspond to normal-tissue complication probability (NTCP) estimates of 2%, 10%, 31%, 61%, and 85%, respectively.

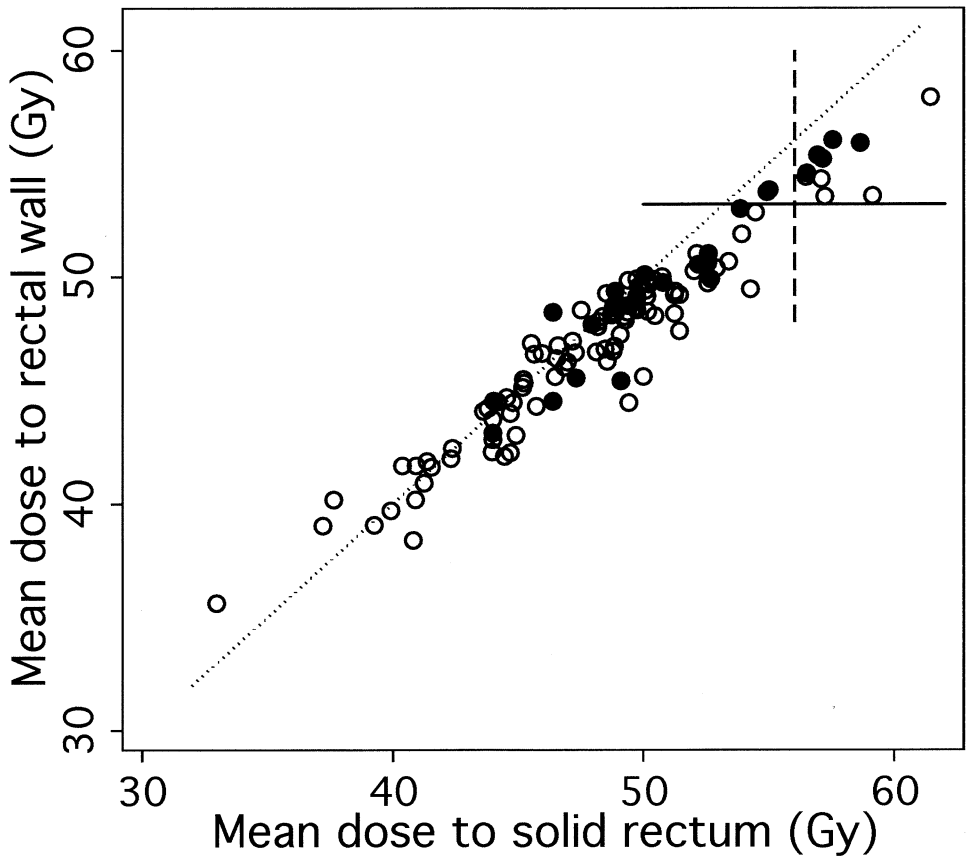

Fig. 6. Mean dose to rectal wall (from the dose wall histogram [DWH]) plotted against mean dose to solid rectum (from the dose volume histogram [DVH]) for each of the 128 patients. Solid symbols indicate patients who experienced Grade 2 or higher late rectal bleeding within 2 years of treatment. The dotted line represents equality of mean dose to solid rectum and rectal wall. The solid line segment represents mean dose to rectal wall of 53.2 Gy; the dashed line segment represents mean dose to solid rectum of 56.0 Gy.

from 8% lower to 10% higher than the mean dose to solid rectum.

In Fig. 6, points to the right of the dashed vertical line segment correspond to patients with mean dose to solid rectum of 56.0 Gy or more, whose estimated risk of late rectal bleeding is 50% or greater, according to the fit of the mean dose model to the DVH data. Of the 10 such patients, 5 actually experienced late rectal bleeding. Points above the solid horizontal line segment had mean doses to rectal wall exceeding 53.2 Gy, which corresponds to a 50% or higher risk of late rectal bleeding based on the fit of the mean-dose model to the DWH data. This subset includes all 10 patients mentioned above, plus 3 additional patients who all experienced late rectal bleeding. Therefore, if NTCP less than 50% is selected as the threshold for predicting late rectal bleeding, the fit of the mean-dose model to the DWH data has a sensitivity of 8/13 = 62% in the present study, compared with a sensitivity of 5/10 = 50% for the fit based on the DVH data. This figure illustrates that although the DWH-based mean-dose model fits the data better than the DVH-based model, the fits are not markedly different.

The results of the present study suggest that patients may be at greater than 50% risk of Grade 2 or higher late rectal bleeding if 80% or more of the rectal wall is exposed to doses as low as 32 Gy, as indicated by the fits of both the cutoff-dose model and the parallel model (Table 2). This conclusion differs from the prevailing view that rectal toxicity is predominantly a consequence of high doses to the portion of anterior rectum adjacent to the prostate gland.

A number of previous studies have supported the prevailing view by demonstrating a significant association between rectal toxicity and volume of rectum exposed to high doses. For example, Boersma *et al.* (2) found that the actuarial incidence of patients with severe bleeding that required one or more laser treatments or blood transfusions (for which the crude incidence was 4 among 130 patients followed for a median of 24 months) was higher among patients with larger percentages of rectal wall exposed to doses of 65 Gy or higher, higher than 70 Gy, or 75 Gy or higher, although no differences were found when toxicity was scored according to the RTOG/EORTC criteria or the SOMA/LENT criteria or scored as bleeding vs. nonbleeding. Using a subset of 89 of the 128 patients analyzed in the present study, Storey *et al.* (13) reported a significantly higher actuarial incidence of Grade 2 or higher late rectal toxicity

among patients with V70 above 25% for solid rectum. Huang *et al.* (9) used data from a larger group ($N = 163$) that included all patients in the present study and reported significant differences in actuarial incidence of Grade 2 or higher late rectal toxicity, depending on V60, V70, V75.6, and V78 values for solid rectum.

In each of the 3 studies cited above, in which high doses to rectum were found to be significantly associated with rectal toxicity, the effects of doses lower than 60 Gy were not reported. Other studies have presented similar findings while considering lower doses as well. Hartford *et al.* (8), for example, reported on a study in which 14 patients had Grade 1 or 2 rectal bleeding among 41 patients treated with a combination of photons and protons and followed for a minimum of 2 years. Significant differences in the crude incidence of rectal bleeding were observed in subgroups of patients dichotomized according to their V60 through V75 values (Cobalt Gy Equivalent), where volumes represent percentages of anterior rectal wall. Differences were not observed for V50 through V58, however. Greco *et al.* (7) used the method of Hartford et al. (8) to analyze RTOG Grade 2 or higher late rectal toxicity (crude incidence 24/135 among patients with follow-up times of 12 to 62 months) for cutoff doses ranging from 7.6 to 79.8 Gy. Significant differences in toxicity were observed for analyses based on V60.8, V68.4, and V72.2 for solid rectum. Wachter *et al.* (14), in a study with 109 patients, analyzed the volumes of rectum receiving doses ranging from 30% to 100% of isodose, which corresponds to doses of approximately 20 to 66 Gy, and found a significant association with RTOG/EORTC Grade 1 or higher late rectal bleeding only for the 90% isodose level, that is, for values corresponding to approximately V59 Gy.

Other previous studies, however, have demonstrated associations between rectal toxicity and the volume of rectum receiving doses less than 60 Gy. Fenwick *et al.* (15) fitted the parallel model to data in which the endpoint was late rectal bleeding within 2 years of treatment (RTOG Grade 0 vs. Grade 1 or higher) among 79 patients with at least 2 years of follow-up and estimated that the sharp rise in the risk of local damage occurs at a dose somewhat less than 60 Gy (i.e., $D_{50} = 57$ Gy). Koper *et al.* (11), in a study of 199 patients who filled out questionnaires regarding the severity of rectal bleeding (none, some, moderate, or severe) at regular hospital visits up to 1 to 3 years posttreatment, found statistically significant differences in actuarial incidence of any rectal bleeding, depending on the volume of rectal wall defined by cutoff doses ranging from 25 to 60 Gy, although with greater significance for higher doses (V60) than for lower doses (V25). On the other hand, Fiorino *et al.* (5) considered volumes of solid rectum ranging from V50 to V75 and found that the actuarial incidence of RTOG Grade 2 or higher late rectal bleeding in a study of 229 patients followed for a median of 30 months was statistically significant for analyses based on V50 through V65, with greater significance at the lower end of the dose range (V50). Cozzarini *et al.* (3) also found, in a study of 128 patients followed for a median of 36 months, that V50 (for solid rectum) was more strongly associated with the time to RTOG Grade 2 or higher late rectal bleeding than volumes defined by larger doses (V60 and V65). Finally, two analyses from the group at Memorial Sloan-Kettering Cancer Center also point to the potential importance of doses less than 60 Gy in causing late rectal bleeding. In those studies, data were analyzed from 49 patients with RTOG Grade 2 or higher late rectal bleeding that occurred within 30 months, plus 122 randomly selected patients who had no rectal bleeding for at least 30 months (10, 12). Logistic regression was used to investigate dose–volume factors related to the incidence of late rectal bleeding, with the variables for each patient weighted to reflect the number of patients who qualified for analysis before data selection. Rectal wall volume was associated with bleeding risk, and for patients with similar volumes of rectal wall, Jackson *et al.* (10) found that the 30-month incidence of rectal bleeding was significantly associated with V46. In a multivariate analysis of the same data by Skwarchuk *et al.* (12), a significant factor for rectal bleeding was whether or not the outer rectal contour was encompassed by the 50% isodose curve on the isocenter CT slice. The prescribed doses to the patients included in the analysis were 70.2 and 75.6 Gy, so the 50% isodose corresponds to doses in the range of 35 to 38 Gy. These doses are very similar to the estimate of 32 Gy suggested by our study to be associated with an increased risk of Grade 2 or higher late rectal bleeding.

At this point, whether the current finding of the importance of the 32-Gy dose level is biologically meaningful for rectal bleeding after prostate radiotherapy is unclear. V32 might have been selected by the model-fitting procedures as optimal because the separation between the average cDWH curves for bleeding and nonbleeding patients is maximal near 32 Gy (Fig. 2a), and not because the biologic effect to rectal tissue actually changes near 32 Gy. Also, V32 might simply be a surrogate for the biologically relevant volume. The relative volumes of rectal wall exposed to different cutoff doses are all highly correlated with one another, and small variations in the data might cause one dose–volume combination to be selected over another just by chance. As noted by Cozzarini *et al.* (3), the DWH is subject to its greatest uncertainty near the maximum dose level, D_{max}, because of organ motion and setup uncertainty, so an intermediate cutoff dose might be selected as a surrogate for D_{max}. On the other hand, others have suggested that injury to the high-dose region might be limited if cellular regeneration occurs in adjacent regions exposed to sufficiently low doses (7, 10, 12). The 32-Gy dose may the dose at which these adjacent regions of rectal wall lose their potential to rescue the most highly dosed areas.

Finally, although we have shown NTCP models to fit the UTMDACC late rectal bleeding data somewhat better when based on dose–volume histograms for rectal wall instead of solid rectum, room for improvement remains. The majority

of patients with late rectal bleeding are not predicted to be at high risk for late rectal toxicity by any of the models considered here. Methods to further improve the prediction of complication risk associated with prostate irradiation are ongoing at our institution, especially by taking organ motion and spatial aspects of the dose distribution into account. By applying an approach similar to that of Hoogeman *et al.* (49), we are attempting to quantify the variations in rectum shape that occur during the course of radiotherapy by obtaining serial CT images on an in-room CT/LINAC system (50). These studies are expected to allow us to obtain better estimates of the actual dose distribution to rectal wall during radiotherapy, which, in turn, may lead to more accurate predictions of rectal tolerance.

REFERENCES

1. Benk VA, Adams JA, Shipley WU, *et al.* Late rectal bleeding following combined X-ray and proton high dose irradiation for patients with stages T3-T4 prostate carcinoma. *Int J Radiat Oncol Biol Phys* 1993;26:551–557.
2. Boersma LJ, van den Brink M, Bruce AM, *et al.* Estimation of the incidence of late bladder and rectum complications after high-dose (70 – 78 Gy) conformal radiotherapy for prostate cancer, using dose-volume histograms. *Int J Radiat Oncol Biol Phys* 1998;41:83–92.
3. Cozzarini C, Fiorino C, Ceresoli GL, *et al.* Significant correlation between rectal DVH and late bleeding in patients treated after radical prostatectomy with conformal or conventional radiotherapy (66.6–70.2 Gy). *Int J Radiat Oncol Biol Phys* 2003;55:688–694.
4. Dale E, Olsen DR, Fosså, SD. Normal tissue complication probabilities correlated with late effects in the rectum after prostate conformal radiotherapy. *Int J Radiat Oncol Biol Phys* 1999;43:385–391.
5. Fiorino C, Cozzarini C, Vavassori V, *et al.* Relationships between DVHs and late rectal bleeding after radiotherapy for prostate cancer: Analysis of a large group of patients pooled from three institutions. *Radiother Oncol* 2002;64:1–12.
6. Fiorino C, Sanguineti G, Cozzarini C, *et al.* Rectal dose-volume constraints in high-dose radiotherapy of localized prostate cancer. *Int J Radiat Oncol Biol Phys* 2003;57:953–962.
7. Greco C, Mazzetta C, Cattani F, *et al.* Finding dose-volume constraints to reduce late rectal toxicity following 3D-conformal radiotherapy (3D-CRT) of prostate cancer. *Radiother Oncol* 2003;69:215–222.
8. Hartford AC, Niemierko A, Adams JA, *et al.* Conformal irradiation of the prostate: Estimating long-term rectal bleeding risk using dose-volume histograms. *Int J Radiat Oncol Biol Phys* 1996;36:721–730.
9. Huang EH, Pollack A, Levy L, *et al.* Late rectal toxicity: Dose-volume effects of conformal radiotherapy for prostate cancer. *Int J Radiat Oncol Biol Phys* 2002;54:1314–1321.
10. Jackson A, Skwarchuk MW, Zelefsky MJ, *et al.* Late rectal bleeding after conformal radiotherapy of prostate cancer (II): Volume effects and dose-volume histograms. *Int J Radiat Oncol Biol Phys* 2001;49:685–698.
11. Koper PCM, Heemsbergen WD, Hoogeman MS, *et al.* Impact of volume and location of irradiated rectum wall on rectal blood loss after radiotherapy of prostate cancer. *Int J Radiat Oncol Biol Phys* 2004;58:1072–1082.
12. Skwarchuk MW, Jackson A, Zelefsky MJ, *et al.* Late rectal toxicity after conformal radiotherapy of prostate cancer (I): Multivariate analysis and dose-response. *Int J Radiat Oncol Biol Phys* 2000;47:103–113.
13. Storey MR, Pollack A, Zagars G, *et al.* Complications from radiotherapy dose escalation in prostate cancer: Preliminary results of a randomized trial. *Int J Radiat Oncol Biol Phys* 2000;48:635–642.
14. Wachter S, Gerstner N, Goldner G, *et al.* Rectal sequelae after conformal radiotherapy of prostate cancer: Dose-volume-histograms as predictive factors. *Radiother Oncol* 2001;59:65–70.
15. Fenwick JD, Khoo VS, Nahum AE, *et al.* Correlations between dose-surface histograms and the incidence of long-term rectal bleeding following conformal or conventional radiotherapy treatment of prostate cancer. *Int J Radiat Oncol Biol Phys* 2001;49:473–480.
16. Li S, Boyer A, Lu Y, *et al.* Analysis of the dose-surface histogram and dose-wall histogram for the rectum and bladder. *Med Phys* 1997;24:1107–1116.
17. Lu Y, Song PY, Li SD, *et al.* A method of analyzing rectal surface area irradiated and rectal complications in prostate conformal radiotherapy. *Int J Radiat Oncol Biol Phys* 1995; 33:1121–1125.
18. MacKay RI, Hendry JH, Moore CJ, *et al.* Predicting late rectal complications following prostate conformal radiotherapy using biologically effective doses and normalized dose-surface histograms. *Br J Radiol* 1997;70:517–526.
19. Meijer GJ, van den Brink M, Hoogeman MS, *et al.* Dose-wall histograms and normalized dose-surface histograms for the rectum: A new method to analyze the dose distribution over the rectum in conformal radiotherapy. *Int J Radiat Oncol Biol Phys* 1999;45:1073–1080.
20. Ting JY, Wu X, Fiedler JA, *et al.* Dose-volume histograms for bladder and rectum. *Int J Radiat Oncol Biol Phys* 1997;38: 1105–1111.
21. Chandra A, Dong L, Huang E, *et al.* Experience of ultrasound-based daily prostate localization. *Int J Radiat Oncol Biol Phys* 2003;56:436–447.
22. Huang E, Dong L, Chandra A, *et al.* Intrafraction prostate motion during IMRT for prostate cancer. *Int J Radiat Oncol Biol Phys* 2002;53:261–268.
23. Lebesque JV, Bruce AM, Guus Kroes AP, *et al.* Variation in volumes, dose-volume histograms, and estimated normal tissue complication probabilities of rectum and bladder during conformal radiotherapy of T3 prostate cancer. *Int J Radiat Oncol Biol Phys* 1995;33:1109–1119.
24. Little DJ, Dong L, Levy LB, *et al.* Use of portal images and BAT ultrasonography to measure setup error and organ motion for prostate IMRT: Implications for treatment margins. *Int J Radiat Oncol Biol Phys* 2003;56:1218–1224.
25. Miralbell R, Özsoy O, Pugliesi A, *et al.* Dosimetric implications of changes in patient repositioning and organ motion in conformal radiotherapy for prostate cancer. *Radiother Oncol* 2003;66:197–202.
26. Nederveen AJ, van der Heide UA, Dehnad H, *et al.* Measurements and clinical consequences of prostate motion during a radiotherapy fraction. *Int J Radiat Oncol Biol Phys* 2002;53: 206–214.
27. Roeske JC, Forman JD, Mesina CF, *et al.* Evaluation of changes in the size and location of the prostate, seminal vesicles, bladder, and rectum during a course of external beam radiation therapy. *Int J Radiat Oncol Biol Phys* 1995;53:1321–1329.
28. Stroom JC, Koper PCM, Korevaar GA, *et al.* Internal organ motion in prostate cancer patients treated in prone and supine position. *Radiother Oncol* 1999;51:237–248.
29. Trichter F, Ennis RD. Prostate localization using transabdominal

ultrasound imaging. *Int J Radiat Oncol Biol Phys* 2003;56:1225–1233.
30. van Herk M, Bruce A, Guus Kroes AP, *et al.* Quantification of organ motion during conformal radiotherapy of the prostate by three dimensional image registration. *Int J Radiat Oncol Biol Phys* 1995;33:1311–1320.
31. Zelefsky MJ, Crean D, Mageras GS, *et al.* Quantification and predictors of prostate position variability in 50 patients evaluated with multiple CT scans during conformal radiotherapy. *Radiother Oncol* 1999;50:225–234,
32. Cheung R, Tucker SL, Ye J, *et al.* Characterization of rectal normal tissue complication probability after high-dose external beam radiotherapy for prostate cancer. *Int J Radiat Oncol Biol Phys* 2004;58:1513–1519.
33. Tucker SL, Cheung R, Dong L, *et al.* Dose-volume-response analyses of late rectal bleeding after radiotherapy for prostate cancer. *Int J Radiat Oncol Biol Phys* 2004;59:353–365.
34. Pollack A, Zagars GK, Starkschall G, *et al.* Prostate cancer radiation dose response: Results of the M.D. Anderson phase III randomized trial. *Int J Radiat Oncol Biol Phys* 2002;53: 1097–1105.
35. Cox JD, Stetz J, Pajak TF. Toxicity criteria of the Radiation Therapy Oncology Group (RTOG) and the European Organization for Research and Treatment of Cancer (EORTC). *Int J Radiat Oncol Biol Phys* 1995;31:1341–1346.
36. Pavy JJ, Denekamp J, Letschert J, *et al.* EORTC late effects working group. Late effects toxicity scoring: the SOMA scale. *Int J Radiat Oncol Biol Phys* 1995;31:1043–1047.
37. Hanlon AL, Schultheiss TE, Hunt MA, *et al.* Chronic rectal bleeding after high-dose conformal treatment of prostate cancer warrants modification of toxicity scales. *Int J Radiat Oncol Biol Phys* 1997;38:59–63.
38. Rasmussen SN, Riis P. Rectal wall thickness measured by ultrasound in chronic inflammatory diseases of the colon. *Scand J Gastroenterol* 1985;20:109–114.
39. Lyman JT. Complication probability as assessed from dose-volume histograms. *Radiat Res* 1985;104(Suppl.):S13–S19.
40. Kutcher GJ, Burman C. Calculation of complication probability factors for non-uniform normal tissue irradiation: The effective volume method. *Int J Radiat Oncol Biol Phys* 1989;16:1623–1630.
41. Mohan R, Mageras GS, Baldwin B, *et al.* Clinically relevant optimization of 3-D conformal treatments. *Med Phys* 1992; 19:933–944.
42. Jackson A, Kutcher GJ, Yorke ED. Probability of radiation-induced complications for normal tissues with parallel architecture subject to non-uniform irradiation. *Med Phys* 1993;20: 613–625.
43. Jackson A, Ten Haken RK, Robertson JM, *et al.* Analysis of clinical complication data for radiation hepatitis using a parallel architecture model. *Int J Radiat Oncol Biol Phys* 1995; 31:883–891.
44. Yorke ED, Jackson A, Rosenzweig KE, *et al.* Dose-volume factors contributing to the incidence of radiation pneumonitis in non-small cell lung cancer patients treated with three-dimensional conformal radiation therapy. *Int J Radiat Oncol Biol Phys* 2002;54:329–339.
45. Morgan BJT. Analysis of quantal response data. New York: Chapman & Hall, 1992.
46. Akaike H. Information theory and an extension of the maximum likelihood principle. In: Petrov BN, Csaki F, editors. Second International Symposium on Information Theory. Budapest: Academiai Kiado; 1973. p. 267–281.
47. Akaike H. A new look at statistical model identification. *IEEE Trans Auto Cont* 1974;19:716–722.
48. Hanley JA, McNeil BJ. The meaning and use of the area under a receiver operating characteristic (ROC) curve. *Radiology* 1982;143:26–36.
49. Hoogeman MS, van Herk M, Yan D, *et al.* A model to simulate day-to-day variations in rectum shape. *Int J Radiat Oncol Biol Phys* 2002;54:615–625.
50. Court L, Rosen I, Mohan R, *et al.* Evaluation of mechanical precision and alignment uncertainties for an integrated CT/LINAC system. *Med Phys* 2003;30:1198–1210.